Astronomy
&
Astrophysics

The very nearby M/T dwarf binary SCR 1845-6357*

M. Kasper[1], B. A. Biller[2], A. Burrows[2], W. Brandner[3], J. Budaj[2,4], and L. M. Close[2]

[1] European Southern Observatory (ESO), Karl-Schwarzschild-Str. 2, 85748 Garching, Germany
   e-mail: `mkasper@eso.org`
[2] Steward Observatory, University of Arizona, 933 North Cherry Avenue, Tucson, AZ 85721, USA
[3] Max-Planck-Institut für Astronomie, Königstuhl 17, 69117 Heidelberg, Germany
[4] Astronomical Institute, Tatranska Lomnica, 05960, Slovak Republic

ABSTRACT

Context. The recently discovered star SCR 1845-6357 (hereafter SCR 1845) is the first late M/T dwarf binary discovered. SCR 1845 is a particular object due to its tight orbit (currently around 4 AU) and its proximity to the Sun (3.85 pc).
Aims. We present spatially resolved VLT/NACO images and low resolution spectra of SCR 1845 in the *J*, *H* and *K* near-infrared bands. Since the T dwarf companion, SCR 1845B, is so close to the primary SCR 1845A, orbital motion is evident even within a year. Following the orbital motion, the binary's mass can be measured accurately within a decade, making SCR 1845B a key T-dwarf mass-luminosity calibrator. The NIR spectra allow for accurate determination of spectral type and also for rough estimates of the object's physical parameters.
Methods. The spectral type of SCR 1845B is determined by direct comparison of the flux calibrated *JHK* spectra with T dwarf standard template spectra and also by NIR spectral indices obtained from synthetic photometry. Constrained values for surface gravity, effective temperature and metallicity are derived by comparison with model spectra.
Results. Our data prove that SCR 1845B is a brown dwarf of spectral type T6 that is co-moving with and therefore gravitationally bound to the M8.5 primary. Fitting the NIR spectrum of SCR 1845B to model spectra yields an effective temperature of about 950 K and a surface gravity $\log g = 5.1$ (cgs) assuming solar metallicity. Mass and age of SCR 1845B are in the range 40 to 50 Jupiter masses and 1.8 to 3.1 Gyr.

Key words. astrometry – stars: late-type – stars: low mass, brown dwarfs – stars: binaries: general

1. Introduction

After decades of little change in the number of known stellar systems in the solar neighborhood, large plate digitization efforts such as the Digitized Sky Survey and SuperCOSMOS (Hambly et al. 2001) as well as surveys like the Two Micron All Sky Survey (2MASS, Skrutskie et al. 2006) have led to the discovery and first order characterisation of numerous previously unknown nearby low mass stars (e.g. Hambly et al. 2004). Many of these stars are very nearby and of low intrinsic luminosity, so they are ideal targets to search for low mass companions, since even a close companion would appear with a reasonably wide separation on the sky and reasonably bright when compared to the primary.

Especially interesting are multiple systems with one component being a main sequence star and at least one other component having a mass below the hydrogen-burning limit, and hence residing in the domain of brown dwarfs. Since all components are expected to be coeval and of the same chemical composition, age and metallicity of the main sequence primary determined by well established methods also applies to the brown dwarf companion. Furthermore, sufficiently tight binary systems would allow one to directly measure the system mass by determining the orbit and even to measure the individual components' masses via monitoring of radial velocities. Hence, the measured luminosity of such

a companion can be used to calibrate effective temperature and surface gravity figures of evolutionary models and provide the required benchmarks.

One such precious benchmark object, Eps Indi B, was resolved into a binary T dwarf (McCaughrean et al. 2004) orbiting the K4.5V primary Eps Indi A during the commissioning of the Simultaneous Differential Imager (SDI, Lenzen et al. 2004; Close et al. 2005) at the VLT. Another T dwarf companion, SCR 1845B, was recently found by Biller et al. (2006) around the M8.5 primary SCR 1845A using the same instrument. SCR 1845 was first reported by Hambly et al. (2004) to be a very red, nearby star at a distance based on plate and 2MASS magnitudes of 3.5 ± 0.7 pc. A little later, Deacon et al. (2005) measured a trigonometric parallax, 282 ± 23 mas, based on SuperCOSMOS photographic plates. This estimate was refined by Henry et al. (2006) who measure a parallax of 259.45 ± 1.11 mas (3.85 ± 0.02 pc), consistent with all previous estimates. Hence, at its distance of 3.85 pc, SCR 1845 is only slightly further away than Eps Indi and the 24th closest star system to Earth known today. This proximity makes SCR 1845B readily accessible to observations despite its small projected separation of only about 4 AU to the primary and its intrinsic faintness.

It is now widely accepted that, besides $T_{\rm eff}$ (a function of bolometric luminosity and radius which are both a function of age), surface gravity (a function of mass and radius) and metallicity have a paramount impact on the spectral energy distribution of late T dwarfs (Gorlova et al. 2003; Liu et al. 2007). Binary
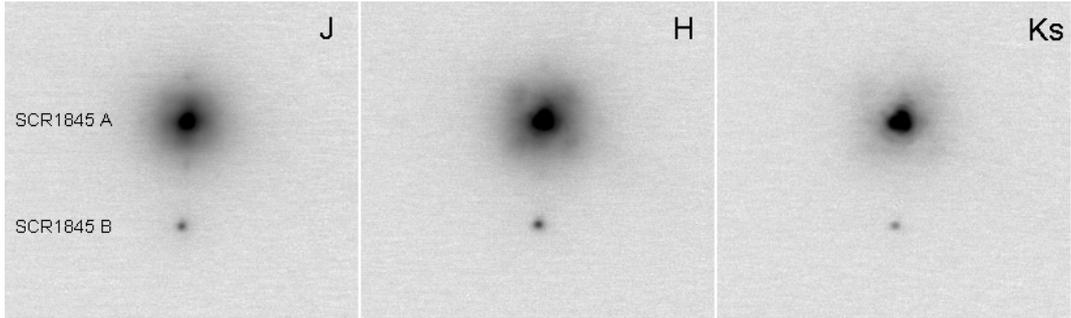
Fig. 1. NACO broad band NIR images of the 1″064 binary SCR 1845 with angular resolution (*FWHM*) of about 67 mas in *J*-, 64 mas in *H*-, and 71 mas in *K*-band. North is up, East is left. Intensities are displayed in a logarithmic scale using identical cut levels in the different bands.

Table 1. Photometry in the 2MASS system and astrometry of SCR 1845A and B.

Object	Date	JD	*J*	*H*	*K*s	Separation	PA
SCR 1845A	2 May 2006	2453858	9.58 ± 0.024	8.99 ± 0.028	8.52 ± 0.022		
SCR 1845B	2 May 2006	2453858	13.26 ± 0.024	13.19 ± 0.028	13.69 ± 0.022	1″064 $\pm$ 0″0038	177°.2 $\pm$ 0°.06
	28 May 2005[a]	2453519		13.16 ± 0.28		1″170 $\pm$ 0″003	170°.2 $\pm$ 0°.13

[a] Biller et al. (2006).

systems that allow us to directly measure as many of these parameters as possible are therefore the key for benchmarking the models and understanding brown dwarf evolution. The mass of SCR 1845 can readily be obtained in the longer term following the orbit which has a period of the order of 20 years (Henry et al. 2006). The individual components' masses can further be determined from additional relative radial velocity measurements. The determination of metallicity and age of late M dwarfs is still rather difficult but a field of active research. Recent methods to derive i) the metallicity of early to mid M dwarfs via atomic (Woolf & Wallerstein 2005) and molecular (Woolf & Wallerstein 2006) indices as well as via absolute magnitudes (Bonfils et al. 2005), and ii) the age of M dwarfs from their chromospheric activity (Silvestri et al. 2005) offer interesting perspectives in this respect.

While Biller et al. (2006) were able to constrain the spectral type of SCR 1845B to T5.5 ± 1, the SDI imaging data did not allow them to deduce a more accurate spectral type and physical properties such as mass, age, metallicity, T_{eff} and L_{bol}. This paper presents follow-up NIR photometry and spectroscopy that is used to accurately determine spectral type by direct comparison to the spectra of T dwarf standards and through spectral indices (Burgasser et al. 2006b), and to further constrain physical properties by direct comparison with modeled brown dwarf spectra (Burrows et al. 1997, 2006). In addition, we also applied a novel method (Burgasser et al. 2006a) for estimating T_{eff} and surface gravity of T dwarfs in the absence of higher resolution spectra.

2. Observations and data reduction

SCR 1845 was observed with NACO mounted on UT4 of the VLT on 2 May 2006. The Adaptive Optics used 90% of the light from the M8.5 primary as a guide star for its infrared wavefront sensor while 10% of the light were directed towards the scientific camera. In this way, we obtained well corrected images that easily resolve the 1″ binary (see Fig. 1).
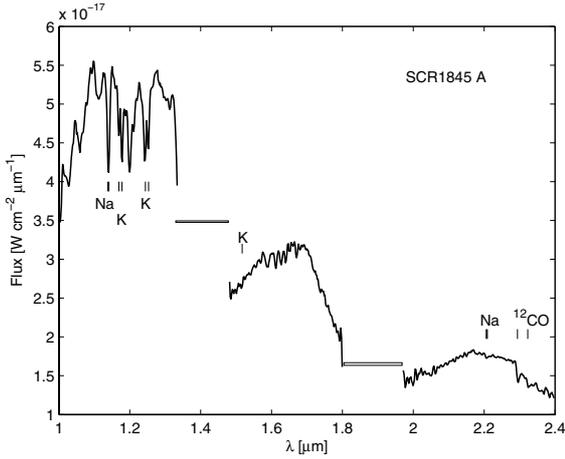
2.1. Imaging

For the imaging observations, the S13 camera of NACO was used in the *J*, *H*- and *K*s near-infrared filters providing a pixel scale of 13.27 mas per pixel. The target was observed with a standard dithering procedure integrating for one minute on source in each of the bands.

Image data reduction followed standard procedures including sky removal, bad pixel cleaning and flat fielding. Differential photometry and astrometry were done on the reduced images with the PSF fitting DAOPHOT package. The primary was used as the PSF for the photometry. We used an iterative procedure in order to attain an accurate PSF. With the original binary image as an initial PSF estimate, the secondary was subtracted out of the image in order to produce a second PSF. This second PSF was then used to attain accurate relative magnitudes for both components of the system differing by less than 3% from initial estimates. The individual magnitudes for SCR 1845A and B were finally calculated from the relative magnitudes and the integrated 2MASS magnitudes of the unresolved system (*J* = 9.54, *H* = 8.97 and *K*s = 8.51, Henry et al. 2004). The error introduced by the difference between NACO and 2MASS instrument response has been calculated from the spectra as described in the next section and has been taken into account. Errors of the astrometric positions were estimated from the standard deviation in the measured separation between the components.

Table 1 displays 2MASS photometry and astrometry of SCR 1845A and B. Given the large proper motion of SCR 1845 of 2″444 RA and 0″696 Dec. per year, the relatively small change in relative position between the two components over the one year between the two measurements confirms the result of Montagnier et al. (2006) and unambiguously proves that SCR 1845 is a bound binary.

2.2. Spectroscopy

After direct imaging on 2 May 2006, NACO was used in long slit spectroscopic mode to obtain $R \approx 400$ spectra in the *J* and *HK* spectroscopic filters (modes S54-4-SJ and S54-4-SHK, 2 nm/px pixel dispersion, S54 camera

Fig. 2. NIR spectrum of SCR 1845A.

Fig. 3. NIR spectrum of SCR 1845B. The underlying gray curve shows the best model fit obtained for $T_{\rm eff} = 950$ K, $\log g = 5.1$ (cgs) and solar metallicity.

Fig. 4. Spectrum of SCR 1845B (black line) plotted on top of T5-7 dwarf spectral standards (normalized to the H band).

Table 2. Spectral indices of SCR 1845B.

H_2O-J	H_2O-H	H_2O-K	CH_4-H	CH_4-K	K/J	K/H
0.155	0.297	0.461	0.286	0.097	0.101	0.221

with 54.3 mas/pixel). By turning the Nasmyth adaptor rotator, the slit was aligned with the binary axis. Dithering the binary at two positions along the slit, exposures of 15 min total in each of the modes were obtained. A telluric calibrator (HIP 95567, spectral type A0V) has been observed in a similar manner just after the object at a similar airmass. A spectrum of the NACO internal Tungsten lamp was recorded for wavelength calibration.

Spectroscopic data reduction followed standard procedures. After sky removal, bad pixel cleaning and flat fielding, the spectra from SCR 1845A and B were extracted and wavelength calibrated. The halo of SCR 1845A at the position of B was estimated by interpolation. The spectra were divided by the telluric calibrator and multiplied by a Kurucz template spectrum of Vega (`http://kurucz.harvard.edu/stars/VEGA/`) smoothed to the actual resolution of the data in order to remove the hydrogen absorption features of the A0V telluric calibrator.
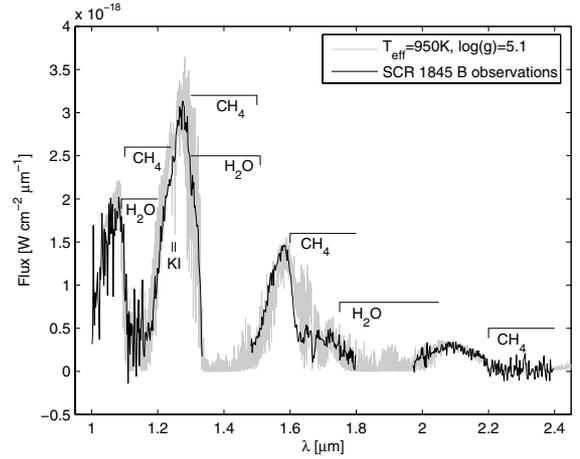
Synthetic magnitudes were calculated from the non-flux calibrated spectra by integrating them over the instrument response curve. The ratio between the synthetic magnitudes of SCR 1845A and B was calculated by integrating the spectra over i) the spectral response of the 2MASS system (Cohen et al. 2003), and ii) the NACO filter response. A comparison between the flux ratios calculated from the same spectra in both photometric systems yields multiplication factors of 1.022 in J, 1.177 in H, and 0.964 in Ks to convert from NACO to 2MASS flux. The rather large correction in H-band originates from the wide NACO filter and the peaked flux distribution of the T dwarf companion in this band, while the M8.5 primary magnitude does not vary much with the assumed photometric system.

Flux calibration of the spectra was finally established using the calculated 2MASS magnitudes of both components (see Table 1) and the 2MASS mag0 flux (Cohen et al. 2003). Figures 2 and 3 show the final NIR spectra of SCR 1845A and B. The figures also indicate the main absorption lines and bands as well as regions of strong telluric absorption.
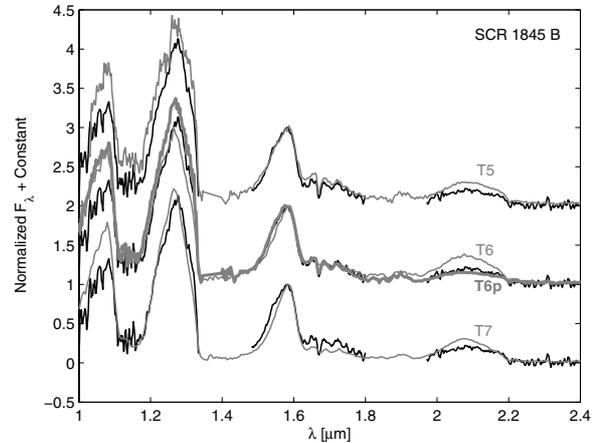
3. Results

3.1. Spectral types

The most direct way to determine the spectral type of a star is direct comparison to spectral standards. Figure 4 plots the NIR spectrum of SCR 1845B (black line) on top of T5-7 dwarf spectral standards (Burgasser et al. 2006b). The T6 standard SDSS 1624+0029 provides a good fit in the J- and H-bands

while the peculiar T6p dwarf 2MASS 0937+2931 better fits the observed K-band flux and leads to a reasonable overall fit. 2MASS 0937+2931 is considered the prototype example of a high surface gravity T dwarf showing the effects of photospheric pressure.

In case a complete NIR spectrum does not exist, the spectral type of SCR 1845B can also be determined from spectral indices. Table 2 shows the indices calculated from the spectra over the wavelength ranges for numerator and denominator defined by Burgasser et al. (2006b). Three (H_2O-J, H_2O-H, CH_4-H) out of the four classification indices are consistent with spectral type T6. Only the CH_4-K index indicates an even later spectral type, but the numerator range of this index ($2.215-2.255$ μm) is in a low SNR part of the spectrum and probably not very reliable.

The NIR spectrum of SCR 1845A agrees with the spectral type M8.5 deduced from optical spectra (Henry et al. 2004). It compares well with the spectrum of LP944-20, an M9V star that has $T_{\rm eff}$ between 2400 K and 2600 K (Basri et al. 2000). The spectrum was further fitted to synthetic spectra calculated with

Table 3. Atomic line equivalent widths (Å) of SCR 1845A and LP 944-20 for comparison. The KI equivalent widths are the sum of the doublets.

Object	KI (1.17 μm)	KI (1.25 μm)	NaI (2.21 μm)
SCR 1845A	15 ± 3	24 ± 3	2 ± 1.2
LP 944-20[a]	14.4 ± 0.6	9.4 ± 0.6	2.7 ± 0.3

[a] Cushing et al. (2005).

the general purpose stellar atmosphere code PHOENIX (Brott & Hauschildt 2005). The best fits were achieved with metallicities $-0.25 < \log Z < 0$ and $2600\,\mathrm{K} < T_{\mathrm{eff}} < 2700\,\mathrm{K}$. Hence, our observations are consistent with SCR 1845A being an M8.5 star, and we adopt an effective temperature of about 2600 K.

Table 3 displays the atomic line equivalent widths of SCR 1845A calculated from its NIR spectrum. The line shape was interpolated using a spline fitting routine, and the continuum was derived by a linear fit to the data points outside the line. Uncertainties on the EWs were estimated from the minimum and maximum acceptable continuum values next to the lines. The measured equivalent widths are comparable to the ones of other stars of similar spectral type presented by Cushing et al. (2005). They do not indicate extreme metallicity or gravity effects.

3.2. Physical parameters of SCR 1845B

We have explored the constraints on T_{eff}, gravity ($\log_{10} g$), and object radius (R) of SCR 1845B due to its overall spectrum shape (in particular the K, J, and H bands flux ratios), its absolute flux levels, and the strength of the KI doublet in its J band. The extracted physical properties are provisional, but reasonable. To fit the observations, first we generated a grid of atmospheric and spectral models for T_{eff} from 800 to 1200 K and for $\log_{10} g$ from 4.75 to 5.5 (cgs). Next, those combinations of T_{eff} and $\log_{10} g$ that reproduced the shape of the observed spectrum, without consideration for the absolute flux level, were determined. Both low-temperature models with low gravities and high-temperatures models with high gravities can fit the shape of the spectrum. In this way, we derived the line in $T_{\mathrm{eff}} - \log_{10} g$ space for which our models fit the spectrum shape. Then, assuming the evolutionary models of Burrows et al. (1997) and Burrows et al. (2006), the *absolute* fluxes, which are functions of mass and age or, alternatively, of T_{eff} and $\log_{10} g$, were fit to the observed absolute flux of SCR 1845B, assuming a distance of 3.85 pc. The result was another line in $T_{\mathrm{eff}} - \log_{10} g$ space, this time one that fits the absolute flux constraint. Hence, using the spectrum shape and the flux separately, two independent lines in $T_{\mathrm{eff}} - \log_{10} g$ space were derived. Naturally, the intersection of these two lines yields a single point that represents the $T_{\mathrm{eff}}/\log_{10} g$ pair that fits best overall. This point is at about $T_{\mathrm{eff}} = 950\,\mathrm{K}$ and $\log_{10} g = 5.1$ (cgs), which are the most probable values of those physical parameters within wide error bars. The procedure described above is similar to the one used by Saumon et al. (2006) to derive the physical properties of the T7.5 dwarf Gliese 570D.

Figure 3 displays the associated model spectrum together with the observed spectrum of SCR 1845B. This fit is for solar metallicity. Lower metallicity would decrease the relative K-band flux, which is also a decreasing function of gravity and an increasing function of temperature. Hence, lower metallicity would tend to shift the best fitting models to slightly higher values of T_{eff}, or slightly lower values of gravity, all else being equal.

Table 4. Parameters of SCR 1845B. First and second columns list possible combinations of the effective temperature (T_{eff}) and radius (R_{fit}) that fit the absolute flux from SCR 1845B. Columns 3–5 list radii from evolutionary models (R_{model}) that correspond to the particular combination of T_{eff} and $\log_{10} g$. Radii that best satisfy both constraints set by the absolute fluxes and evolutionary models are those with $R_{\mathrm{fit}} \approx R_{\mathrm{model}}$ and are printed in bold.

T_{eff}	R_{fit} (10^{10} cm)	R_{model} (10^{10} cm)		
		$\log g = 5$	$\log g = 5.25$	$\log g = 5.1$
800	0.94	0.654	0.589	
900	0.72	0.662	0.597	
950	0.63	0.666	0.601	**0.639**
1000	0.58	0.670	**0.604**	
1100	0.47	0.677	0.610	
1200	0.40	0.684	0.616	

Finally, we calculated profiles of the KI doublet at 1.25 μm in the J band. These lines are barely discernible in the observed spectrum, but are present in most of our synthetic spectra. The model equivalent widths decrease towards lower T_{eff} and higher gravities. This is because the 1.25 μm KI doublet requires high excitation temperatures. Higher gravities place this high-temperature region at higher pressures and depths, thereby progressively burying it. So, if we were to weight our conclusions by the constraint imposed by the shallow KI doublet, we would shift our derived T_{eff} and gravities accordingly. An interpretation of the weakness of these lines in the observed spectrum might also be that the potassium abundance is subsolar. However, given the otherwise good overall fit the metallicity itself is not appreciably subsolar.

Simultaneous correlated constraints on T_{eff} and radius of SCR 1845B can be obtained using the absolute flux level. Table 4 lists the possible combinations, along with model radii. A consistent model for T_{eff} and radius is obtained at $T_{\mathrm{eff}} = 950-1000\,\mathrm{K}$, and $R \approx 0.63 \times 10^{10}$ cm ($0.88\,R_J$). This is also consistent with $\log_{10} g = 5.1-5.25$ and spectral type T6p. Using the Burrows et al. (1997) evolutionary models, we find mass/age pairs that are more or less consistent with the spectral fits of ($41\,M_J$, 1.8 Gyr), ($51\,M_J$, 3.1 Gyr), and ($51.8\,M_J$, 2.6 Gyr), with a very slight preference for the first pair.

An approximate estimate of T_{eff} and $\log g$ can also be derived from spectral indices (Burgasser et al. 2006a). Applying this method using the indices given in Table 2, we find that the phase spaces of H$_2$O-J and K/H do not intersect assuming solar metallicity and staying inside the $\log g < 5.5$ limit (Burrows et al. 1997). However, since both H$_2$O-J and K/H are more sensitive to metallicity than to surface gravity (Liu et al. 2007), only slightly subsolar metallicities are needed to find a valid combination of T_{eff} and $\log g$ which would reasonably well agree with the results from the direct fit of the model to the spectrum.

It is also interesting to compare SCR 1845B to the T6 dwarf ϵ Indi Bb, which as part of the Ba/Bb binary system, is one of the two most nearby (3.626 pc) brown dwarfs known today. Both NACO NIR photometry and H-band spectrum of ϵ Indi Bb (McCaughrean et al. 2004) are very similar to our SCR 1845B data. The absolute J, H and Ks magnitudes of the two objects differ by less than 0.1 mag from each other, with SCR 1845B being slightly brighter and bluer. The H-band spectra are virtually identical. Based on their data and assuming an age of 2 Gyr, McCaughrean et al. (2004) used the bolometric correction BC$_K$ presented by Golimowski et al. (e.g. 2004) and the Burrows et al. (1997) evolutionary models to derive a mass of $38\,M_J$ for

ϵ Indi Bb. This result is a rather good match to our estimate of SCR 1845B's mass.

4. Conclusions

Following up the discovery of SCR 1845B, we have obtained J, H and Ks imaging and spectroscopy of the SCR 1845 binary. Given the large proper motion of SCR 1845, the relatively small $(0.1'')$ change in relative position of the two stars between 2005 and 2006 confirms that the binary system is gravitationally bound. With only two data points available no further constraints on orbital parameters can be set for now.

Comparison with spectral standards and PHOENIX model fitting indicate spectral type M8.5 and $T_{\mathrm{eff}} \approx 2600\,\mathrm{K}$ for the primary SCR 1845A as already derived before from the optical spectrum. A similar procedure using spectral standards and the University of Arizona evolutionary models for Brown dwarfs yields spectral type T6, $T_{\mathrm{eff}} \approx 950\,\mathrm{K}$ and $\log g \approx 5.1$ (cgs) for SCR 1845B. Considering also its measured luminosity, mass and age of SCR 1845B can be constrained to 40 to 50 Jupiter masses and 1.8 to 3.1 Gyr. SCR 1845B further exhibits strong K-band suppression and weak KI lines at $1.25\,\mu$m both indicative of either high surface gravity or low metallicity. Hence, further dedicated observation of SCR 1845B might help us to obtain a better understanding of the complex interaction of surface gravity and metallicity in the formation of brown dwarf spectra.

The similarity between J, H, K absolute magnitudes and H-band spectrum of SCR 1845B and ϵ Indi Bb is striking. Both T6 dwarfs have a main sequence companion and will have accurately measured masses (from measuring the orbital motion of SCR 1845AB and Eps Indi Ba-Bb) on time scales of a few years. Further high-resolution NIR spectroscopy and astrometry of SCR 1845B will therefore allow us to directly measure its mass and to constrain its physical parameters such as metallicity and age. This makes SCR 1845B one of the few precious objects known today that has the potential to provide the required benchmarks for testing evolutionary models.

References

Basri, G., Mohanty, S., Allard, F., et al. 2000, ApJ, 538, 363
Biller, B. A., Kasper, M., Close, L. M., Brandner, W., & Kellner, S. 2006, ApJ, 641, L141
Bonfils, X., Delfosse, X., Udry, S., et al. 2005, A&A, 442, 635
Brott, I., & Hauschildt, P. H. 2005, in ESA SP-576: The Three-Dimensional Universe with Gaia, ed. C. Turon, K. S. O'Flaherty, & M. A. C. Perryman, 565
Burgasser, A. J., Burrows, A., & Kirkpatrick, J. D. 2006a, ApJ, 639, 1095
Burgasser, A. J., Geballe, T. R., Leggett, S. K., Kirkpatrick, J. D., & Golimowski, D. A. 2006b, ApJ, 637, 1067
Burrows, A., Marley, M., Hubbard, W. B., et al. 1997, ApJ, 491, 856
Burrows, A., Sudarsky, D., & Hubeny, I. 2006, ApJ, 640, 1063
Close, L. M., Lenzen, R., Guirado, J. C., et al. 2005, Nature, 433, 286
Cohen, M., Wheaton, W. A., & Megeath, S. T. 2003, AJ, 126, 1090
Cushing, M. C., Rayner, J. T., & Vacca, W. D. 2005, ApJ, 623, 1115
Deacon, N. R., Hambly, N. C., & Henry, T. J. E. A. 2005, AJ, 129, 409
Golimowski, D. A., Leggett, S. K., Marley, M. S., et al. 2004, AJ, 127, 3516
Gorlova, N. I., Meyer, M. R., Rieke, G. H., & Liebert, J. 2003, ApJ, 593, 1074
Hambly, N. C., MacGillivray, H. T., & Read, M. A. E. A. 2001, MNRAS, 326, 1279
Hambly, N. C., Henry, T. J., Subasavage, J. P., Brown, M. A., & Jao, W.-C. 2004, AJ, 128, 437
Henry, T. J., Subasavage, J. P., & Brown, M. A. E. A. 2004, AJ, 128, 2460
Henry, T. J., Jao, W.-C., Subasavage, J. P., et al. 2006, AJ, 132, 2360
Lenzen, R., Close, L., Brandner, W., Biller, B., & Hartung, M. 2004, in Ground-based Instrumentation for Astronomy, ed. A. F. M. Moorwood, & I. Masanori, Proc. SPIE, 5492, 970
Liu, M. C., Leggett, S. K., & Chiu, K. 2007, ArXiv Astrophysics e-prints
McCaughrean, M. J., Close, L. M., & Scholz, R.-D. E. A. 2004, A&A, 413, 1029
Montagnier, G., Ségransan, D., Beuzit, J.-L., et al. 2006, A&A, 460, L19
Saumon, D., Marley, M. S., Cushing, M. C., et al. 2006, ApJ, 647, 552
Silvestri, N. M., Hawley, S. L., & Oswalt, T. D. 2005, AJ, 129, 2428
Skrutskie, M. F., Cutri, R. M., et al. 2006, AJ, 131, 1163
Woolf, V. M., & Wallerstein, G. 2005, MNRAS, 356, 963
Woolf, V. M., & Wallerstein, G. 2006, PASP, 118, 218